Cost-benefit Analysis of Transmission Network Reliability Standards: An Inverse Optimal Power Flow Approach

Felipe Sepúlveda[a,c,1], Diego Alvarado[b,c], Felipe Cordera[d], Eduardo Esperguel[e], Goran Strbac[f], Rodrigo Moreno[b,c].

[a] Department of Industrial Engineering, University of Chile, Santiago, 8370456, Chile
[b] Department of Electrical Engineering, University of Chile, Santiago, 8320000, Chile
[c] Instituto Sistemas Complejos de Ingeniería (ISCI), Santiago, 8370398, Chile
[d] Operation Research Center, Massachusetts Institute of Technology, Cambridge, MA 02139, USA
[e] National Energy Commission, Santiago, 8340518, Chile
[f] Department of Electrical and Electronic Engineering, Imperial College London, London, SW7 2AZ, UK

Keyword: Inverse optimization, Reliability, Supply continuity metrics, Reliability parameters

Abstract

The provision of reliable and cost-effective electricity supply is vital for modern societies. Achieving this balance between reliability and cost can be explored through stochastic optimization models. However, these models are often perceived by practitioners as overly complex, intractable and demanding extensive, often unavailable, reliability data. This paper presents a novel approach: the inverse optimization problem of the probabilistic security-constrained optimal power flow (PSC-OPF). This method enables the determination of missing outage and repair rates of network components, aligning with observed supply continuity levels. By integrating the determined (or calibrated) outage and repair rates into a transmission network expansion planning model, we assess the impacts of network investments on enhancing supply continuity levels. We employ machine learning, decomposition and regularization approaches to manage large-scale instances of stochastic problems. Through a real-world application to the Chilean power system, we demonstrate that our proposed inverse model's calibration leads to more accurate, realistic, and credible results that then can be used to appropriately plan network investments. Our results informed the setting and upgrading of the transmission network reliability standards in Chile, resulting in substantial cost savings and supply continuity enhancements for the electricity consumers.

1. Introduction

Ensuring a reliable and cost-effective electricity supply to consumers is critical in power systems. At the transmission system level, the application of reliability criteria has been the predominant reason to undertake network investments (Joskow, 2006). However, these reliability criteria were developed

[1] Corresponding author's email: felisepulveda@ug.uchile.cl.

several decades ago and are usually justified based on engineering judgement rather than on appropriate cost-benefit analysis.

The right balance between costs and benefits associated with reliability network standards can be studied through two-stage stochastic optimization models (Strbac, Kirschen, & Moreno, 2016). In these models, investments in new network capacity (determined at the first stage) continue until the cost outweighs the benefits of improved reliability, measured by reduced demand curtailment and enhanced supply continuity (determined at the second stage). While the power industry often acknowledges the benefits of probabilistic analysis and stochastic models for making investment decisions to enhance reliability, these models are also viewed as overly complex and difficult to implement on a real-scale network. Moreover, they require extensive amounts of often unavailable reliability data. In this context, this paper features two chief contributions:

- We introduce the **inverse optimization problem** for the probabilistic security-constrained optimal power flow (PSC-OPF), a novel approach that allows us to determine missing reliability data (i.e., outage and repair rates of network components) required to align with observed supply continuity levels.
- We solve a series of stochastic optimization problems—specifically, the proposed inverse PSC-OPF problem, the PSC-OPF problem, and the probabilistic transmission expansion planning problem—on the real-world transmission network of Chile, which includes 2,200 lines and transformers, and 2,400 buses. To manage the large-scale instances of these problems, we employ various techniques such as machine learning, decomposition, and regularization approaches.

Our analysis has led to the formulation of a new network reliability standard, which has been successfully adopted by the Chilean authority since 2020. This standard, the first to be developed through operations research, achieves an optimal balance between reliability levels and network investment costs, contributing to enhanced supply continuity to the best possible tariff.

This paper is organized as follows. Section 2 provides the conceptual framework and introduces the inverse PSC-OPF model. Section 3 outlines the solution strategy for the inverse optimization problem. Sections 4 and 5 detail the real-world application of a network investment model for enhancing reliability in the Chilean system, relying on our model's calibration. Section 6 presents the results that inform the 2020 security standards by the National Energy Commission (NEC) in Chile. Finally, Section 7 concludes by highlighting the impact of our work.

2. The Background and Proposed Inverse OPF Problem

In this chapter, we establish the conceptual framework for our work by introducing the optimization models traditionally used to study power systems' reliability. We begin with a description of the well-known Optimal Power Flow (OPF) problem, followed by its extensions that incorporate reliability considerations, based on either robust (deterministic) or probabilistic (stochastic) concepts. We also demonstrate the application of these formulations to both operation and investment problems. We emphasize that probabilistic models are sensitive to the reliability parameters of network components, such as failure and repair rates, as these determine outage probabilities. In this context, we propose an inverse optimization model that calibrates the reliability parameters of network components. This calibration ensures that the (forward) OPF models with probabilistic security accurately reflect the supply continuity levels experienced by consumers, thereby producing appropriate results.

2.1. The Optimal Power Flow Problem and Its Extensions

The OPF problem is a mathematical program that determines the flows through the network components (e.g., lines and transformers) and power output of generators, so demand is supplied at minimum cost while satisfying physical constraints (Stott & Alsac, 2012) (Cain, O'Neill, & Castillo, 2012). The aim of the OPF model is usually to determine optimal system operation for a single operating condition (i.e., a snapshot or timeslice), which can be a normal (also called pre-contingency) condition or a contingency (also called post-contingency) condition. The pre-contingency operation can be planned in a robust fashion to hedge the system against unplanned outages of components, adjusting the operating variables in the normal condition to remain within safe ranges during contingencies without the need to shed demand. These adjustments, known as *preventive* actions, can be obtained through additional constraints in the OPF problem to ensure security margins for facing system contingencies. On the other hand, *corrective* actions are those applied after the outage occurs and aim at minimizing its impact. They can include delivering generation reserves, switching transmission lines, and utilizing power-flow controlling devices, such as phase-shifting transformers and high voltage direct current systems (Hedman, O'Neill, Fisher, & Oren, 2009) (Chen, Moreno, Strbac, & Alvarado, 2018).

When pre- and post-contingency operations are jointly modeled in the OPF problem to ensure that there are no demand disconnections post-contingency, the model is known as the Security-Constrained Optimal Power Flow (SC-OPF) problem (Monticelli, Pereira, & Granville, 1987), which is a robust optimization program formulated as follows (see details in Appendix A of version used in paper):

$$\min_{x_0, x_s} \quad c_0(x_0) \tag{1.a}$$

$$s.t. \quad a_0(x_0) \geq b_0, \tag{1.b}$$

$$a_s(x_s) \geq b_s, \qquad \forall s = 1,\ldots,C, \tag{1.c}$$

$$\|x_0 - x_s\| \leq \Delta_s, \qquad \forall s = 1,\ldots,C, \tag{1.d}$$

where x_0 represents pre-contingency operating decisions (i.e., during the "normal" system state, without outages), and x_s represents corrective actions under the s-th contingency. The objective function (1.a) corresponds to the operational cost during normal conditions. Constraints (1.b) and (1.c) respectively model restrictions associated with system operation in the normal state and during each one of the C contingency scenarios. Constraints (1.d) capture the flexibility of corrective actions, limited by the parameter Δ_s.

The SC-OPF problem guarantees the security of supply across a range of contingencies deemed as "credible" (typically those associated with the N-1 or N-2 criteria, which involve any single or double outage, respectively; in the context of robust optimization, this represents the uncertainty set), thus providing a robust solution for the operation problem. However, the resulting reliability levels depend on the set of contingencies being considered instead of stemming from a balance of the cost and benefits of the preventive actions required to provide reliability (He, Cheng, Kirschen, & Sun, 2011).

The stochastic counterpart of the aforementioned robust program is known as the Probabilistic Security-constrained Optimal Power Flow (PSC-OPF) model. This model is a standard mathematical tool used to quantify the effects of network outages on supply interruptions. It operates as a two-stage stochastic program that minimizes the expected operational cost of the system under normal conditions and across various contingency scenarios. In the first stage, the program determines pre-contingency operational decisions. In the second stage, it addresses system operation under each contingency, which may include demand interruptions at different locations. This approach balances the costs and benefits of preventive and corrective actions, thereby achieving optimal reliability levels from an economic perspective. The PSC-OPF is formulated as follows (Capitanescu, et al., 2011) (see details in Appendix B of version used in paper):

$$\min_{x_0, x_s, y_s} \quad p_0 c_0(x_0) + \sum_{s=1}^{M} p_s c_s(x_s, y_s) \tag{2.a}$$

$$s.t. \quad a_0(x_0) \geq b_0, \tag{2.b}$$

$$a_s(x_s, y_s) \geq b_s, \qquad \forall s = 1,\ldots,M, \tag{2.c}$$

$$\|x_0 - x_s\| \leq \Delta_s, \qquad \forall s = 1,\ldots,M, \tag{2.d}$$

which has a similar structure to the SC-OPF but presents two significant differences. Firstly, variables y_s are introduced to permit load shedding during the post-contingency operation. Secondly, the objective function (2.a) considers operating cost during the normal state and the expected cost of corrective actions during contingency scenarios, including demand curtailments, which allows to evaluate whether it is convenient to leave unsupplied energy in some scenarios if the required preventive actions to avoid it are too costly. In addition, the number of contingencies considered in the PSC-OPF, denoted by M, is usually higher than those of the SC-OPF (denoted by C), as the impact of each contingency is weighted by its probability. Using expected costs allows for the consideration of outage scenarios beyond those deemed credible.

The previous PSC-OPF formulation can be readily extended to include network investment decisions in its first stage (Krishnan, et al., 2016) (Zhang, Vittal, Heydt, & Quintero, 2012), thus modifying pre- and post-contingency actions by increasing transmission capacity. In addition, the investment costs must be considered in the objective function of the problem. This extended model is stated as follows (Strbac, Kirschen, & Moreno, 2016) (see details in Appendix C of version used in paper):

$$\min_{x_0,x_s,y_s,z} \quad c_I(z) + p_0 c_0(x_0) + \sum_{s=1}^{M} p_s c_s(x_s,y_s) \tag{3.a}$$

$$s.t. \quad a_I(z) \geq b_I, \tag{3.b}$$

$$a_0(x_0,z) \geq b_0, \tag{3.c}$$

$$a_s(x_s,y_s,z) \geq b_s, \qquad \forall s = 1,\ldots,M, \tag{3.d}$$

$$\|x_0 - x_s\| \leq \Delta_s, \qquad \forall s = 1,\ldots,M, \tag{3.e}$$

where z is the vector of investment decisions, whose costs c_I are reflected in the objective function (3.a). Constraints (3.b) define the set of feasible investment options, which may be limited in physical or budgetary terms. The remaining restrictions are interpreted the same way as before, with (3.c) and (3.d) explicitly recognizing their dependency on investment decisions.

2.2. Our Proposed Inverse Probabilistic Security-constrained Optimal Power Flow

The outage and repair rates of network components (also referred to as reliability parameters) are critical inputs in probabilistic models as they determine the probability of each contingency scenario. However, accurately determining these values is extremely challenging in practice.

While reliability parameters can be estimated from historical data, these records are often incomplete and inaccurate (Rodrigues & Silva, 2013), leading to suboptimal decisions when identifying cost-effective investments to enhance system reliability. For instance, (Alvarado, Moreira, Moreno, & Strbac, 2018) highlight the impact of inaccurate reliability data on investment decisions in transmission expansion

planning. Additionally, aging processes and inadequate maintenance can alter the outage probability of components over time, which may require reliability data to be updated in a timely fashion (Alvarado, Moreno, Orchard, & Kirschen, 2022). Furthermore, climate-driven events and other natural hazards can affect reliability data (Panteli & Mancarella, 2015). All these factors make it challenging to reliably estimate outage and repair rates.

Unlike the reliability parameters of transmission assets, supply continuity data has been made readily available as regulators usually monitor the quality of supply closely (i.e., interruptions frequency and duration, and the volume of unsupplied energy). In this context, our work proposes a novel methodology that uses inverse optimization to find reliability parameters of network components based on known supply continuity metrics. This approach leverages the straightforward availability of supply continuity data, allowing us to calibrate the PSC-OPF problem to reflect the actual supply continuity levels perceived by consumers. Consequently, this enhances the PSC-OPF model's ability, and its extended version that plans network investments, to inform effective alternatives for improving reliability levels.

Importantly, our proposed method calculates reliability parameters with a systemwide perspective rather than on a component-by-component basis, providing a coherent solution aligned with observed continuity metrics. This is a significant advantage, as alternative methods that determine reliability data at the component level, by inferring outage and repair rates from historical performance, often lack a systemwide perspective and alignment with the continuity levels perceived by consumers, making their results less credible in practice. The inverse PSC-OPF (also referred to as the "inverse" problem) is formulated as follows:

$$\min_{r,\epsilon} \quad \sum_{j=1}^{J} \alpha_j \|\epsilon_j\| \qquad (4.a)$$

$$s.t. \quad h_j(r) - q_j = \epsilon_j, \quad \forall j = 1,\ldots,J, \qquad (4.b)$$

$$r \in [\underline{r},\bar{r}], \qquad (4.c)$$

where r is a vector containing the reliability parameters of the PSC-OPF (namely, the outage and repair rates of network components), h_j represent mathematical expressions for the supply continuity metrics (e.g., duration, frequency, and volume of interruptions) at different buses, while q_j correspond to the respective observed metrics, and ϵ_j quantifies the associated errors between the calibrated and observed values. The objective function (4.a) minimizes the weighted sum of calibration errors, where the weights α_j express the relative importance of each metric to be calibrated, whose values might be determined using expert knowledge. Constraints (4.b) compute each error, while (4.c) restricts the calibrated

reliability parameters to lie within prespecified ranges, thus allowing the search to be conducted only in the vicinity of prior estimates (e.g., derived from the available, albeit poor, historical data).

A related problem to the abovementioned inverse PSC-OPF is presented by (Hu, Xie, & Tai, 2018) and (Niu, et al., 2021), under the name of Inverse Power System Reliability Evaluation. They formulate an analytical model based on nonlinear algebraic equations to obtain the unknown reliability parameters using a set of specified reliability indices. Their scope, however, is limited to the case where the number of unknown parameters equals the number of selected indices, which allows the set of nonlinear equations to be solved numerically. In this vein, our work presents a more general framework to estimate (or calibrate) the reliability parameters. Remarkably, as our approach is based on optimization, it allows for a much simpler inclusion of additional constraints, which are often needed for specific applications in the power industry.

Finally, it is important to note that even in the hypothetical case where reliability parameters are fully available, using them in the PSC-OPF model may not necessarily lead to the supply continuity effects observed in practice. This is because models, even large-scale and real-world ones like those used in this work, are always idealized and simplified versions of reality. Therefore, a systemwide calibration process not only addresses the issue of unavailable data but also mitigates errors induced by model simplifications. This aspect is critically important when working with practitioners, as they expect the model (and its input parameters) to accurately replicate observed effects before proceeding further.

3. The Proposed Methodology for Calibration via Inverse Optimization

In this chapter, we further explore the inverse PSC-OPF problem described in equations (4.a) - (4.c), providing the necessary definitions for power system reliability modeling and the analytical expressions for the supply continuity metrics of interest. Next, we discuss a preprocessing step that prepares the data by clustering it to make the model more tractable and avoid overfitting. Finally, we present the solution strategy for the proposed inverse optimization problem.

3.1. Analytical expressions of the supply continuity metrics h_j

We use a Markov process to represent the transitions between the different states of the system, which allow us to determine the h_j metrics as explained in (Billington & Allan, 1984). That is, for each asset i, the availability A_i and unavailability U_i are calculated using its reliability parameters, specifically the outage λ_i and repair μ_i rates, through the following expressions:

$$A_i = \frac{\mu_i}{\lambda_i + \mu_i}; U_i = \frac{\lambda_i}{\lambda_i + \mu_i}. \qquad (5)$$

Then, the probability p_s of each system state s (or scenario s) is calculated as follows:

$$p_s = \prod_{i \in \mathcal{B}_s^{up}} A_i \prod_{i \in \mathcal{B}_s^{dw}} U_i \,, \qquad (6)$$

where $\mathcal{B}_s^{up}$ and $\mathcal{B}_s^{dw}$ are the sets of available and unavailable components, respectively, under the system state s. In this paper, we use the following h_j metrics: System Average Interruption Frequency Index (SAIFI) [occurrences], System Average Interruption Duration Index (SAIDI) [hours], and Expected Energy Not Supplied (EENS) [MWh], whose analytical expressions are:

$$SAIDI_j = \sum_{s \in \mathcal{S}_j^{ls}} p_s \cdot T \,, \qquad (7.a)$$

$$SAIFI_j = \sum_{s \in \mathcal{S}_j^{ls}} F_{sj} = \sum_{s \in \mathcal{S}_j^{ls}} \sum_{k \in \mathcal{S}_j^{0}} p_k \cdot r_{ks}, \qquad (7.b)$$

$$EENS_j = \sum_{s \in \mathcal{S}_j^{ls}} p_s \cdot L_{sj} \cdot T. \qquad (7.c)$$

Notice that T refers to the duration of the representative operating condition (e.g., if a year is represented by a single timeslice, T equals 8760 hours), F_{sj} the frequency at which the system state s is reached from any other state without load shedding $\mathcal{S}_j^0$ in node j, r_{ks} the transition between states k and s by using λ_i or μ_i as appropriate, and L_{sj} the load shedding for each system state s and node j. The states with and without load shedding $\mathcal{S}_j^{ls}$ and $\mathcal{S}_j^0$, together with the amounts of load shedding L_{sj}, will be determined by two OPF models, as explained later (Figure 1).

3.2. Implementation Strategy: Preprocessing data and the solution strategy

The proposed methodology is applied through a two-step process. The first step involves preprocessing data, where the machine learning technique known as *decision trees* is used to cluster demand nodes and network assets into groups. Given that outages are infrequent, historical records can be inaccurate or biased due to the limited dataset. Therefore, we use groups rather than individual data avoiding overfitting to individual (and potentially inaccurate) values. Additionally, clustering data into groups enhances the model's tractability.

The second step involves solving the inverse PSC-OPF model, described in equations (4.a) - (4.c), using a metaheuristic approach. This approach determines the reliability parameters of network components that replicate the supply interruption levels observed in historical data. Below, we explain these steps in more detail.

3.2.1. Clustering buses and assets

Buses: We aim to form Ψ groups of (comparable) buses sharing similar topological and electrical features, and where the variance of supply continuity metrics within each cluster ψ is minimal. To achieve this, we use *decision trees*, which predict the value of a target variable (in this case, a supply continuity metric like SAIFI, SAIDI or EENS) by learning simple decision rules inferred from data features. These rules shape the branches of the decision tree, ultimately defining each cluster. We use the following four features to characterize each bus:

- Radiality: Indicates whether the node is connected to a radial or meshed part of the network. A node's connection is considered radial if there is a single branch or circuit connecting it to the rest of the system, meaning there are no loops. In the radial case, this metric reflects the distance between the node and the closest meshed piece; otherwise, it is zero.
- Connectivity: The number of branches that are incident to the node (i.e., degree or valency).
- Voltage: The voltage level of the node.
- Distributed generation: The aggregated capacity embedded in the node.

We expect nodes connected to a meshed piece of the transmission network, with high connectivity and voltage levels, and a larger capacity of distributed generation, to feature improved supply continuity levels. Other features could be used as well, depending on the case and available data. This approach also enhances model tractability as it reduces the number of h_j metrics.

Assets: The lack of richer outage data may lead to substantially different reliability parameters across network components, even for comparable ones. This motivates sharing the same outage and repair rates (per unit of length, in the case of lines) within assets of the same class. We define a class according to the component type, its voltage level, and location (e.g., transmission lines of 220 kV located in a given zone are assumed to feature the same reliability data). In our study, this feature is highly desirable for the power industry as differences in reliability data for similar assets are difficult to justify in practice. This approach also enhances model tractability as it reduces the number of outage and repair rates to be calibrated. Depending on the application, these classes may be defined according to other features as well (e.g., the aging of components).

3.2.2. The solution strategy to solve the inverse optimization problem

We use three concatenated optimization programs to solve (4.a) - (4.c) and determine the network components' outage and repair rates that reproduce the historical levels of the supply continuity metrics (Figure 1). First, we run a SC-OPF problem to determine the pre- and post-contingency operation for each timeslice, aiming to replicate the system operator's dispatches of generators for every operating

condition. Over this pre-contingency operation fixed, we simulate a higher set of contingencies to identify in which scenarios load is disconnected and by how much, which is necessary to determine $h_j(r)$ metrics (e.g., SAIDI, SAIFI and EENS, for different groups of nodes). Finally, we use an Adaptive Differential Evolution metaheuristic (Zhang & Sanderson, 2009) to solve (4.a) - (4.c), which is suitable for non-convex problems like ours.

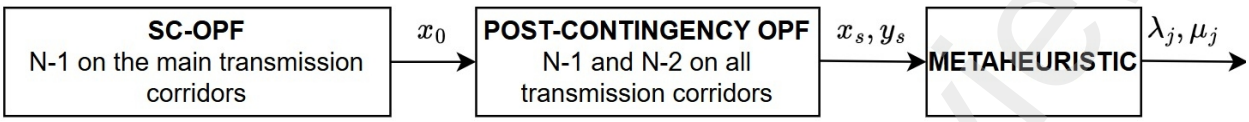

Figure 1. Calibration process diagram.

The metaheuristic starts with an initial population of *individuals*, each representing a solution to the inverse problem (i.e., a set of λ_i and μ_i values for each asset class), randomly generated within a prespecified range. Subsequently, through *crossover* and *mutation* operators, new individuals are created, and the initial population evolves according to a selection criterion based on a *fitness function* f_{sc} (namely, the inverse problem's objective) that captures the adjustment errors ϵ_j relative to the historical metrics q_j. The process stops when the errors are less than or equal to a given tolerance or a maximum number of iterations is reached.

Specifically, we consider target metrics at two aggregation levels: systemic (i.e., all demand nodes) and clusters of nodes. Thus, the objective function is stated as follows:

$$f_{sc} = \alpha_{sys}\|\epsilon_{sys}\| + \sum_{\psi \in \Psi} \alpha_{\psi}\|\epsilon_{\psi}\|, \quad (8)$$

where ϵ_{sys} and ϵ_{ψ} denote the respective errors, and α values are the associated weights.

4. The application: Network Investments for Reliability Enhancements

4.1. Pure cost-benefit balance

In this work, the calibrated reliability parameters are used to determine the optimal set of investments in transmission infrastructure to mitigate the impact of outages on system operations, thereby improving the supply continuity levels perceived by consumers. To achieve this, we use the model stated in equations (3.a) - (3.e). Given the application of this formulation to a very large-scale instance, we employ decomposition and regularization techniques, along with additional methods detailed below.

For Benders decomposition, we follow the approach in (Moreno, Pudjianto, & Strbac, 2013), where investment and pre-contingency operation decisions are included in the master problem, while the post-contingency operations are handled by a set of subproblems that can be solved in parallel. Each subproblem determines post-contingency operations given the investment and pre-contingency operation proposals determined by the master problem.

Regarding the regularization technique, we apply a variant of the method proposed by (Asamov & Powell, 2018), which introduced quadratic regularization as a term in the objective function that penalizes deviations of state variables from their values in the previous iteration. This term diminishes as iterations progress. Our variant differs in that we use the absolute-value distance instead of the Euclidean distance to maintain linearity, as explained in (Cordera, Moreno, & Ordóñez, 2023). Additionally, computational complexity is further reduced by decoupling network investment decisions in radial and meshed transmission assets, as the interaction between both is minimal.

4.2. Target supply continuity levels

Another feature of our model is the inclusion of SAIDI and SAIFI metrics as linear functions of EENS within the set of constraints. We constructed these linear functions using linear regression analysis to enable setting bounds for these metrics. Thus, the model not only identifies the portfolio of network investments that optimally balances the costs of investments and unsupplied demand, but it also determines the portfolio of network investments that achieves target supply continuity levels in each node at minimum cost. This approach serves to analyse the Chilean energy policy outlined in the country's Energy Roadmap (Ministerio de Energia Chile, 2015), which sets explicit annual outage duration limits for each node.

It is important to mention that Benders decomposition cannot handle bounds on the supply continuity metrics per node. Therefore, to find network enhancements that allow the system to respect these bounds, we first determine the optimal investment portfolio from a pure cost-benefit balance point of view (as in the previous section). With these assets fixed, we then run the monolithic investment model (without decomposition) with bounds on the supply continuity metrics to add further investments to the portfolio solution. This two-step approach significantly reduces computational times.

5. Case Studies and Input Data

We run one central case study and several sensitivities. The central case study determines the optimal set of network investments justified due to a cost-benefit balance between (i) the investment (including maintenance) costs of the new network infrastructure and (ii) the corresponding reductions in the expected cost of energy not supplied (i.e., supply continuity improvements). Then, we run several sensitivities that, rather than freely balancing these costs, impose a given supply continuity target for all nodes, determining the optimal network enhancements that comply with such target. We run the model for a wide range of targeted values of SAIDI, from 0.15h to 40h. The same SAIDI value is applied to all demand nodes simultaneously. We use SAIDI as a targeted metric of continuity of supply as it is consistent with the energy policy agenda in Chile. Before running the above case studies, we calibrate network

components' reliability parameters using the method proposed in this paper, demonstrating that the model can deliver credible results for the power industry.

The most relevant considerations in terms of input data, assumptions, and modeling are:

- We use a 2400-bus representation of the Chilean transmission system (545 demand nodes, 450 generators, 1298 lines, and 869 transformers).
- Demand per node, parameters of generators (capacities and costs), and the network topology mentioned above correspond to those used and published by the Chilean system operator (Coordinador Electrico Nacional, Documentos de modelacion del SEN, 2019).
- Investment and maintenance costs of network components are taken from the Regulated Asset Value report published by the regulatory authority for tariff purposes (Ministerio de Energia Chile, 2017).
- The value of the lost load is equal to $12,960/MWh (Ministerio de Energia Chile, 2018).
- For potential investments, we consider candidate network components so every branch in the network complies with the N-1 redundancy criterion: 1,002 candidate lines and 225 candidate transformers. Today, only a fraction of the transmission network complies with it.
- We restrict our study to contingencies consisting of single or double outages (for the case of lines in the same circuit). This is motivated by the nature of potential investments considered.
- Prior estimates associated with the reliability parameters of network components are taken from estimations by the Chilean system operator. We only consider data associated with forced outages under milder events as planned outages and extreme events are ignored when SAIDI, SAIFI, and EENS are measured (Coordinador Electrico Nacional, 2018).
- The network companies report SAIDI, SAIFI, and EENS in all demand nodes to the Chilean regulatory office. We use the data available between 2012 and 2018.
- All studies are carried out for the present system condition (2019) to avoid investments due to demand growth. Hence, investments can be justified only due to reliability benefits (i.e., post-contingency congestion relief). We also add further constraints in the pre-contingency operation to mimic actual power transfer limits applied by the system operator and thus obtain credible results for the power industry (Coordinador Electrico Nacional, 2018).

6. Results and Discussion

6.1. Calibration

As outlined in Section 3, we cluster the network buses (or nodes) into groups based on their features such as radiality, connectivity, voltage and volumes of distributed generation in different locations of the system. Then, we calibrate the reliability data for each asset class to match the modeled and observed

supply continuity data, specifically the systemwide SAIDI, and the SAIDI and SAIFI of each node group. Importantly, to achieve these results, the errors in SAIDI and SAIFI for each cluster (i.e., modeled minus observed historical values) were minimized to zero, resulting in a perfect calibration by adjusting the outage and repair rates starting from the prior estimates. The resulting calibrated failure and repair rates are depicted in Figure 2, showing that transformers have a lower failure frequency than lines. Additionally, as expected, lines with higher voltages fail less frequently since higher voltage towers are more robust.

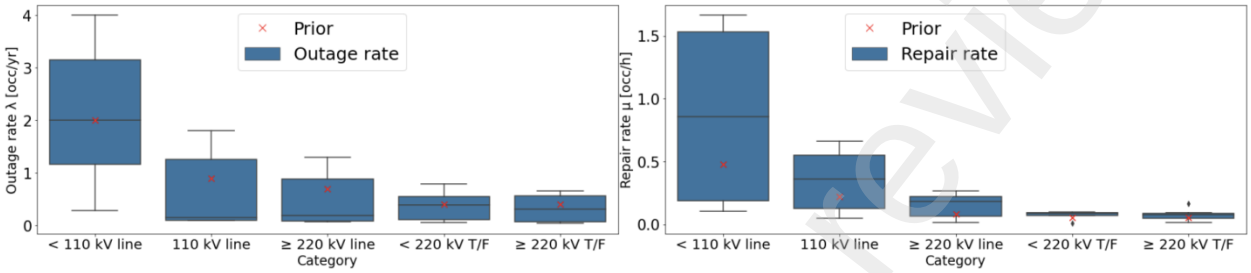

Figure 2: Failure rates and repair rates of component classes (per 100 km lines and transformers; T/F refers to transformers). The given prior estimates are presented in red color.

Figure 2 also shows significant variance in the reliability performance of network assets within the same class, suggesting that local characteristics (e.g., environment and climate) and their particular state of health (due to aging and maintenance policies) significantly affect reliability data. The large differences between the calibrated rates and their prior estimates highlight the importance of our proposed calibration method, as without it, a single prior value would be used for all assets in the same class, potentially leading to inaccurate assessments.

6.2. Balancing Investment Costs and Reliability Enhancements

After calibrating the failure and repair rates, we proceed to enhance the transmission network. The optimal solution for the transmission expansion planning problem, which balances investment and unsupplied energy costs, involves $24.2M in annuitized investment costs. This results in $97.5M in savings from the expected costs of energy not supplied, yielding a net benefit of $73.3M. Notably, the expected energy not supplied is halved, and the systemwide SAIDI and SAIFI are significantly reduced by 48% and 25%, respectively. About 65% of the investment costs are allocated to building new lines, covering approximately 1000 km. Additionally, the model installs about 1.7 GW in 25 new transformers. These results are shown in Table 1.

Table 1. Results of optimal investments (M$ refers to millions of dollars).

Investments in lines	No. lines	48
	Aggregated length [km]	1,041
	Capacity [MW]	2,316
	Investment cost (lines) [M$/yr]	15.7
Investments in transformers	No. transformers	25
	Capacity [MW]	1,765
	Investment cost (transformers) [M$/yr]	8.5
Cost-benefit balance	Investment cost (total) [M$/yr]	24.2
	Expected cost of energy not supplied (reduction) [M$/yr]	97.5
	Expected net benefit [M$/yr]	73.3
Systemwide supply continuity metrics	EENS (before – after investments) [GWh/yr]	(14 – 7)
	SAIDI (before – after investments) [h/yr]	(2.3 – 1.2)
	SAIFI (before – after investments) [occ/yr]	(1.3 – 1)

From a policymaker's perspective, a critical issue with the above optimal solution is the uneven distribution of reliability levels across the network. Figure 3 shows the distribution of nodal SAIDIs before and after the investments. Although there is a significant improvement in the systemwide SAIDI (a 48% reduction), local SAIDI remains poor for several buses. In Figure 3, dots with high SAIDI represent nodes usually located far from the main meshed system and with small demand levels. In these areas, installing redundancies is costlier than the corresponding savings in the expected cost of energy not supplied. We address this "equity" problem in the next section.

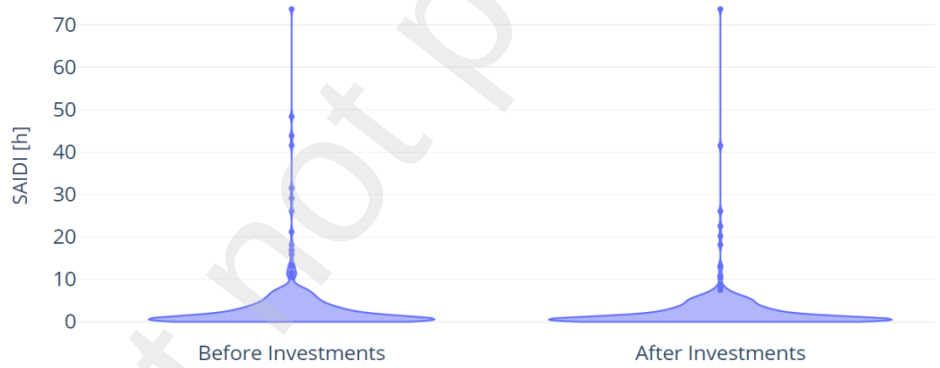

Figure 3. Distribution of SAIDI across the nodes pre- and post-investment.

6.3. Reliability-constrained Investments: Improving Worst-served Areas

In this section, we study target reliability levels per node by enforcing an upper bound on the SAIDI levels across all nodes. Figure 4 shows the annuitized investment costs associated with imposing different upper bounds on SAIDI.

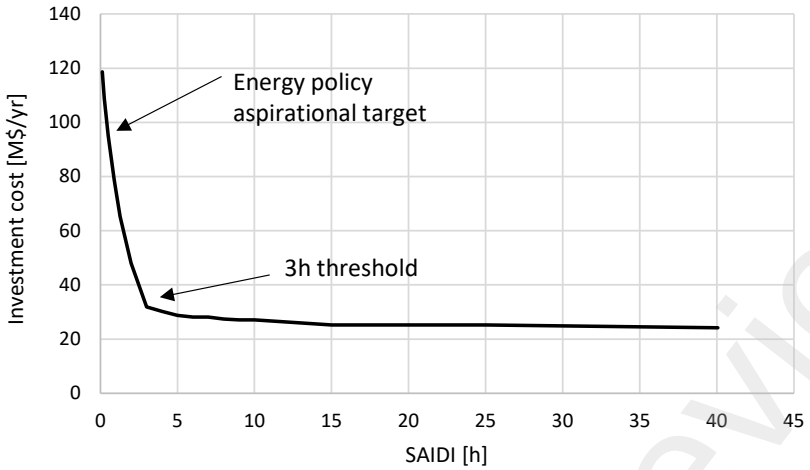

Figure 4. Annuitized investment cost as a function of SAIDI's upper bound applied on all nodes.

Expectedly, more stringent reliability levels drive higher costs. For instance, the aspirational energy policy target of 0.5 hours leads to an investment cost of $95.1M per year, significantly higher than the optimal investment cost found in the previous section ($24.2M). Interestingly, imposing a SAIDI limit of up to 3 hours on every node appears to be a reasonable compromise between costs and policy aspirations, as investment costs escalate considerably below this threshold.

Finally, it is essential to highlight that improving reliability beyond the levels shown in Table 1 and imposing arbitrary reliability targets may result in disproportionately high network costs and thus tariffs. Additionally, our results demonstrate that these improvements are mainly undertaken in rural areas, where increasing tariffs may be particularly complicated due to the consumers' socio-economic backgrounds. Cross-subsidies may likely be needed to support more equitable and fairer solutions regarding the distribution of supply continuity levels among network users.

7. Conclusions and impacts of this work

This paper introduces a novel inverse optimization approach for the PSC-OPF problem, enabling the determination of missing reliability data to align with observed supply continuity levels. We apply this method to the real-world transmission network of Chile, solving various stochastic optimization problems, including the probabilistic transmission expansion planning problem. We showcase advanced techniques such as machine learning, decomposition, and regularization to effectively manage large-scale instances. Our results significantly influenced the development of Chile's transmission network reliability standards in two chief ways. First, we demonstrated, from a pure cost-benefit analysis perspective, that further network investments were necessary and beneficial. We identified specific investments totalizing $24.2 million per year in annuitized value, which would reduce expected energy not supplied cost by $97.5 million per year, resulting in a net benefit of $73.3 million per year for the consumers of the entire national

power system. Secondly, we showed that the costs of meeting certain policy targets were disproportionate to their benefits. Instead, we proposed adopting a 3-hour SAIDI target per node, which was incorporated into the new network security standard enacted by NEC in 2020.

Importantly, the models developed in this paper were provided to NEC staff during the formulation of the standards. In fact, NEC significantly contributed to the results presented in this paper. The process also involved roundtable discussions among academia, government, and industry, where the models played a critical role in testing different hypotheses, informing the debate, and shaping the final standards.

Appendix A. SC-OPF

The formulation described here falls within the framework of an SC-OPF and represents the starting point of more complex formulations used in counter-security operation planning. More specifically, for each contingency scenario, a short-term instant of operation is modelled (i.e. a short-term post-contingency snapshot). In this, it is assumed that the generation units, due to their technical ramping limitations, can only dispatch the reserves determined in the pre-contingency stage, representing the corrective actions, and, furthermore, the safe transfer limits for the flows are relaxed. Additionally, decisions to turn on and off generation units are incorporated in the pre-contingency state, enriching the set of preventive actions available to the system. Finally, to model reality more reliably, line losses are incorporated. All the parameters and decision variables of the model, together with the mathematical formulation, are then presented:

Sets and indices

I: Set of all assets of system i (transmission lines and transformers).

N: Set of all nodes n of the system.

S: Set of all contingency scenarios s, including the pre-contingency state ($s = 0$).

G: Set of all generation units g of the system.

Z: Set of all geographical zones z into which the system is divided.

G_n: Set of all the generation units g installed in node n.

G_z: Set of all the g generation units installed in geographical zone z.

ST: Set of all the groups of secure assets st that share the same secure transfer limit.

Parameters

$to(l)$: Indicates the node n towards which line l enters.

$fr(l)$: Indicates the node n from which line l exits.

M: Very large constant used for angular decoupling of failed assets.

$\overline{F}_l$: Thermal limit for line l [MW].

P_g^{max},P_g^{min}: Maximum and minimum generation limits respectively for unit g [MW].

$r_g^{up,max}$,$r_g^{down,max}$: Maximum and minimum reserve limits respectively for unit g [MW].

LST_{st}: Safe transfer limit for the safe asset group st.

R_z^{up},R_z^{down}: Minimum reserve limits up and down respectively, for geographical area z [MW].

D_n: Power demand at node n [MW].

FC_g: Capacity factor of generation unit g.

FP: Loss factor over the network representing a percentage of the installed capacity of the system, distributed among all assets susceptible to loss.

x_l: Reactance of line l [ohm].

$length(l)$: Length of line l.

u: Minimum length threshold [km] of an asset i for it to present losses.

CV_g: Variable cost for generation unit g [$/MWh].

CR_g^{up},CR_g^{down}: Cost of maintaining up and down reserves respectively for unit g [$/MWh].

Decision variables

$p_{g,0}$: Power generated for unit g in the pre-contingency state [MW].

$f_{l,0}$: Power flow through line l in the pre-contingency state [MW].

$f_{l,0}^{pos}$,$f_{l,0}^{neg}$: Power flows through line l in the pre-contingency state [MW], necessary to define the losses.

$\theta_{l,0}$: Phase angle for line l in the pre-contingency state [rad].

$r_{g,0}^{up}$,$r_{g,0}^{down}$: Up and down reserves for unit g in the pre-contingency state [MW].

$x_{g,0} = \begin{cases} 1, & if\ unit\ g\ is\ on\ in\ the\ pre-contigency\ state. \\ 0, & otherwise. \end{cases}$

$p_{(g,s)}$: Power generated for unit g of scenario s in the post-contingency condition [MW].

$f_{(l,s)}$: Power flow through line l of scenario s in the post-contingency condition [MW].

$f_{(l,s)}^{pos}$,$f_{(l,s)}^{neg}$: Power flow through line l of scenario s in the post-contingency condition [MW], necessary to define the losses.

$\theta_{(l,s)}$: Phase angle for line l of scenario s in the post-contingency condition [rad].

Mathematical formulation

$$\underset{\substack{p_{(g,s)},f_{(l,s)},f_{(l,s)}^{pos},\\ f_{(l,s)}^{neg},\theta_{(l,s)},r_{(g,0)}^{up},\\ r_{(g,0)}^{down},x_{(g,0)}}}{\text{Min}} \sum_{g\in G} CV_g p_{g,0} + CR_g^{up} r_{g,0}^{up} + CR_g^{down} r_{g,0}^{down} \tag{A.1}$$

$$\sum_{g\in G_n} p_{g,s} + \sum_{l\in L|to(l)=n} f_{l,s} = D_n + \sum_{l\in L|fr(l)=n} f_{l,s} + \frac{1}{2} \sum_{\substack{l\in L|(to(l)=n \\ \vee fr(l)=n) \\ \wedge length(l)\geq u}} FP\left(f_{l,s}^{pos} + f_{l,s}^{neg}\right), \forall n \in N, \forall s \in S, \tag{A.2}$$

$$-M\widehat{a_{l,s}} + \frac{1}{x_l}(\theta_{fr(l),s} - \theta_{to(l),s}) \leq f_{l,s} \leq \frac{1}{x_l}(\theta_{fr(l),s} - \theta_{to(l),s}) + M\widehat{a_{l,s}}, \forall l \in L, \forall s \in S, \tag{A.4}$$

$$f_{l,s} = f_{l,s}^{pos} - f_{l,s}^{neg}, SOS1\left(f_{l,s}^{pos}, f_{l,s}^{neg}\right), \forall l \in L, \forall s \in S, \tag{A.3}$$

$$-(1 - \widehat{a_{l,s}})\overline{F}_l \leq f_{l,s} \leq \overline{F}_l(1 - \widehat{a_{l,s}}), \forall l \in L, \forall s \in S, \tag{A.5}$$

$$-LST_{st} \leq \sum_{l\in st} f_{l,0} \leq LST_{st}, \forall st \in ST, \tag{A.6}$$

$$p_{g,0} + r_{g,0}^{up} \leq P_g^{max} x_{g,0} FC_g, \forall g \in G, \tag{A.6}$$

$$p_{g,0} - r_{g,0}^{down} \geq P_g^{min} x_{g,0}, \forall g \in G, \tag{A.7}$$

$$0 \leq r_{g,0}^{up} \leq r_g^{up,max}, \forall g \in G, \tag{A.8}$$

$$0 \leq r_{g,0}^{down} \leq r_g^{down,max}, \forall g \in G, \tag{A.9}$$

$$\sum_{g\in z} r_{g,0}^{up} \geq R_z^{up}, \forall z \in Z, \tag{A.11}$$

$$\sum_{g\in z} r_{g,0}^{down} \geq R_z^{down}, \forall z \in Z, \tag{A.12}$$

$$p_{g,0} - r_{g,0}^{down} \leq p_{g,s} \leq p_{g,0} + r_{g,0}^{up}, \forall g \in G, \forall s \in S\backslash\{0\}, \tag{A.13}$$

$$x_{g,0} \in \{0,1\}, \forall g \in G, \tag{A.14}$$

where (A.1) represents the objective function to minimize, which considers the operating costs in the pre-contingency state, (A.2)-(A.5) represent the energy balance (A.2) and angular coupling (A.3) constraints at each node, and the losses (A.4) and thermal limits (A.5) on the transmission lines, for all contingency scenarios including the pre-contingency state, (A.6) represents the safe transfer limits for transmission lines in the pre-contingency state, (A.7)-(A.12) model the generation and reserve limit constraints for the pre-contingency state, (A.13) represents the corrective action constraints, and finally (A.14) sets as binary variables the switching on and off of generation units.

Appendix B. PSC-OPF

This model corresponds to an extension of the SC-OPF described in Appendix A, where an additional medium-term post-contingency snapshot is incorporated. In this, a re-dispatch similar to the pre-contingency one is solved, however, being a fault state, no reserves are kept and no safe transfer limits are imposed, but there is flexibility to reallocate the running generators, representing the corrective actions. In addition, the costs and benefits of preventive and corrective actions are balanced in the objective function, quantifying the cost of unsupplied demand through the incorporation of a load disconnection variable in both snapshots, further imposing that this should be lower in the medium-term snapshot due to the flexibility allowed. For the formulation of this model, additional definitions are needed:

Sets and indices

Y: Set of all snapshots y, where $y = 1$ and $y = 2$ represent the short- and medium-term post-contingency snapshots respectively, while $y = 0$ represents a snapshot for the pre-contingency state, which is only defined to allow for a more compact notation of the model.

$\mathbb{A}$: Set of all combinations of indices (s,y) except $(s = 0 \wedge y > 0) \wedge (s > 0 \wedge y = 0)$.

Parameters

$VoLL$: Cost of energy not supplied [$/MWh].

β_y: Calibration weight for the post-contingency snapshot y.

$\hat{a}_{l,s} = \begin{cases} 1, & if\ the\ asset\ l\ is\ failed. \\ 0, & otherwise. \end{cases}$

$\mathrm{P}(\hat{a}_s)$: probability of occurrence of contingency s (previously defined in Section 3).

Decision variables

$L_{(n,s,y)}$: Load shedding at node n of scenario c in the post-contingency snapshot y [MW] (previously defined in Section 3).

Mathematical formulation

$$\min_{\substack{p_{(g,s,y)},f_{(l,s,y)},\\ f^{pos}_{(l,s,y)},f^{neg}_{(l,s,y)},\\ \theta_{(l,s,y)},L_{(n,s,y)},x_{g,s,y},\\ r^{up}_{(g,s,y)},r^{down}_{(g,s,y)}}} \sum_{s\in S} \mathrm{P}(\hat{a}_s) \sum_{y\in Y} \beta_y \left[\sum_{g\in G} CV_{g,s,y} p_{g,s,y} + CR^{up}_g r^{up}_{g,s,y} + CR^{down}_g r^{down}_{g,s,y} + \sum_{n\in N} VoLL\, L_{n,s,y} \right], \tag{B.1}$$

$$\sum_{g\in G_n} p_{g,s,y} + \sum_{l\in L|to(l)=n} f_{l,s,y} = D_n + \sum_{l\in L|fr(l)=n} f_{l,s,y} - L_{n,s,y} + \frac{1}{2} \sum_{\substack{l\in L|(to(l)=n\\ \vee fr(l)=n)\\ \wedge length(l)\geq u}} FP\left(f^{pos}_{l,s,y} + f^{neg}_{l,s,y}\right), \forall n\in N, s\in S, y\in Y, (s,y) \tag{B.2}$$

$$-M\widehat{a_{l,s}} + \frac{1}{x_l}\left(\theta_{fr(l),s,y} - \theta_{to(l),s,y}\right) \leq f_{l,s,y} \leq \frac{1}{x_l}\left(\theta_{fr(l),s,y} - \theta_{to(l),s,y}\right) + M\widehat{a_{l,s}}, \forall l\in L, s\in S, y\in Y, (s, \tag{B.3}$$

$$f_{l,s,y} = f^{pos}_{l,s,y} - f^{neg}_{l,s,y}, SOS1\left(f^{pos}_{l,s,y}, f^{neg}_{l,s,y}\right), \forall l\in L, s\in S, y\in Y, (s,y)\in \mathbb{A}, \tag{B.4}$$

$$-(1-\widehat{a_{l,s}})\overline{F}_l \leq f_{l,s,y} \leq \overline{F}_l(1-\widehat{a_{l,s}}), \forall l\in L, s\in S, y\in Y, (s,y)\in \mathbb{A}, \tag{B.5}$$

$$-LST_{st} \leq \sum_{l\in st} f_{l,0,0} \leq LST_{st}, \forall st\in ST, \tag{B.6}$$

$$p_{g,0,0} - r^{down}_{g,0,0} \leq p_{g,s,y} \leq p_{g,0,0} + r^{up}_{g,0,0}, \forall g\in G, s\in S\backslash\{0\}, y\in Y\backslash\{2\}, (s,y)\in \mathbb{A}, \tag{B.7}$$

$$0 \leq L_{n,s,y} \leq D_n, \forall n\in N, s\in S, y\in Y\backslash\{2\}, (s,y)\in \mathbb{A}, \tag{B.8}$$

$$0 \leq L_{n,s,y} \leq L_{n,s,1}, \forall n\in N, s\in S\backslash\{0\}, y\in Y\backslash\{1\}, (s,y)\in \mathbb{A}, \tag{B.9}$$

$$L_{n,0,0} = 0, \forall n\in N, \tag{B.10}$$

$$P^{min}_g x_{g,s,y} \leq p_{g,s,y} \leq P^{max}_g x_{g,s,y} FC_g, \forall g\in G, s\in S\backslash\{0\}, y\in Y\backslash\{1\}, (s,y)\in \mathbb{A}, \tag{B.11}$$

$$p_{g,0,0} + r^{up}_{g,0,0} \leq P^{max}_g x_{g,0,0} FC_g, \forall g\in G, \tag{B.12}$$

$$p_{g,0,0} - r^{down}_{g,0,0} \geq P^{min}_g x_{g,0,0}, \forall g\in G, \tag{B.13}$$

$$0 \leq r^{up}_{g,0,0} \leq r^{up,max}_g, \forall g\in G, \tag{B.14}$$

$$0 \leq r^{down}_{g,0,0} \leq r^{down,max}_g, \forall g\in G, \tag{B.15}$$

$$r^{up}_{g,s,y} = 0, \forall g \in G, s \in S \backslash \{0\}, \in Y \backslash \{0\}, \quad \text{(B.16)}$$

$$r^{down}_{g,s,y} = 0, \forall g \in G, s \in S \backslash \{0\}, \in Y \backslash \{0\}, \quad \text{(B.17)}$$

$$\sum_{g \in z} r^{up}_{g,0,0} \geq R^{up}_{z}, \forall z \in Z, \quad \text{(B.18)}$$

$$\sum_{g \in z} r^{down}_{g,0,0} \geq R^{down}_{z}, \forall z \in Z, \quad \text{(B.19)}$$

$$x_{g,s,y} \in \{0,1\}, \forall g \in G, s \in S, y \in Y \backslash \{1\}, (s,y) \in \mathbb{A}, \quad \text{(B.20)}$$

where (B.1) represents the objective function to be minimized, which is weighted by the probability of contingencies, and considers the pre-contingency state operating costs plus the cost of corrective actions of the short (reserve dispatch) and medium term (generation unit reallocation) weighted post-contingency snapshot, (B.2) represents the nodal balancing constraint with load shedding, (B.8) represents the maximum allowed load shedding limit, (B.9) models the fact that the increased flexibility in the medium-term snapshot causes the load shedding to be lower than that obtained in the short-term snapshot, and (B.10), (B.16), and (B.17), represent consistency constraints due to the use of compact notation. All other restrictions are the same as those presented in Appendix A.

Appendix C. PSC-OPF planning problem

This model corresponds to an extension of the PSC-OPF described in Appendix B, where the cost of new network infrastructure is quantified in the objective function, through the incorporation of a decision variable to determine reliability-justified network investments. For the formulation of this model, additional definitions are needed:

Sets and indices

I: Set of all candidate network assets i.

Parameters

c^{Inv}_{i}: Cost of new network asset i [$].

Decision variables

$$v_i = \begin{cases} 1, & if\ active\ candidate\ i\ is\ installed. \\ 0, & otherwise. \end{cases}$$

Mathematical formulation

$$\min_{\substack{p_{(g,s,y)},f_{(l,s,y)},\\ f^{pos}_{(l,s,y)},f^{neg}_{(l,s,y)},\\ \theta_{(l,s,y)},\Delta D_{(n,s,y)},x_{g,s,y},\\ r^{up}_{(g,s,y)},r^{down}_{(g,s,y)},v_i}} \sum_{i\in I} c_i^{Inv} v_i + \sum_{s\in S} \mathrm{P}(\hat{a}_s) \sum_{y\in Y} \beta_y \left| \sum_{g\in G} CV_{g,s,y} p_{g,s,y} + CR_g^{up} r^{up}_{g,s,y} + CR_g^{down} r^{down}_{g,s,y} + \sum_{n\in N} VoLL\, L_{n,s,y} \right|, \tag{C.1}$$

$$\sum_{g\in G_n} p_{g,s,y} + \sum_{l\in L|to(l)=n} f_{l,s,y} + \sum_{i\in I|to(i)=n} f_{i,s,y} = D_n + \sum_{l\in L|fr(l)=n} f_{l,s,y} + \sum_{i\in I|fr(i)=n} f_{i,s,y} - L_{n,s,y} + \frac{1}{2} \sum_{\substack{l\in L|(to(l)=n \\ \vee fr(} \\ \wedge lengt} \tag{C.2}$$

$$\left(f^{pos}_{l,s,y} + f^{neg}_{l,s,y}\right) + \frac{1}{2} \sum_{\substack{i\in I|(to(i)=n \\ \vee fr(i)=n) \\ \wedge length(i)\geq u}} FP\left(f^{pos}_{i,s,y} + f^{neg}_{i,s,y}\right), \forall n \in N, s \in S, y \in Y, (s,y) \in \mathbb{A},$$

$$-M\widehat{a_{l,s}} + \frac{1}{x_l}\left(\theta_{fr(l),s,y} - \theta_{to(l),s,y}\right) \leq f_{l,s,y} \leq \frac{1}{x_l}\left(\theta_{fr(l),s,y} - \theta_{to(l),s,y}\right) + M\widehat{a_{l,s}}, \forall l \in L, s \in S, y \in Y, (s, \tag{C.3}$$

$$f_{l,s,y} = f^{pos}_{l,s,y} - f^{neg}_{l,s,y}, SOS1\left(f^{pos}_{l,s,y}, f^{neg}_{l,s,y}\right), \forall l \in L, s \in S, y \in Y, (s,y) \in \mathbb{A}, \tag{C.4}$$

$$-(1-\widehat{a_{l,s}})\overline{F}_l \leq f_{l,s,y} \leq \overline{F}_l(1-\widehat{a_{l,s}}), \forall l \in L, s \in S, y \in Y, (s,y) \in \mathbb{A}, \tag{C.5}$$

$$-LST_{st} \leq \sum_{l\in st} f_{l,0,0} \leq LST_{st}, \forall st \in ST, \tag{C.6}$$

$$-M(1-v_i) + \frac{1}{x_i}\left(\theta_{fr(i),s,y} - \theta_{to(i),s,y}\right) \leq f_{i,s,y} \leq \frac{1}{x_i}\left(\theta_{fr(i),s,y} - \theta_{to(i),s,y}\right) + M(1-v_i), \forall i \in I, s \in S \in Y, (s,y) \in \mathbb{A}, \tag{C.7}$$

$$f_{i,s,y} = f^{pos}_{i,s,y} - f^{neg}_{i,s,y}, SOS1\left(f^{pos}_{i,s,y}, f^{neg}_{i,s,y}\right), \forall i \in I, s \in S, y \in Y, (s,y) \in \mathbb{A}, \tag{C.8}$$

$$-v_i\overline{F}_i \leq f_{i,s,y} \leq \overline{F}_i v_i, \forall i \in I, s \in S, y \in Y, (s,y) \in \mathbb{A}, \tag{C.9}$$

$$p_{g,0,0} - r^{down}_{g,0,0} \leq p_{g,s,y} \leq p_{g,0,0} + r^{up}_{g,0,0}, \forall g \in G, s \in S\backslash\{0\}, y \in Y\backslash\{2\}, (s,y) \in \mathbb{A}, \tag{C.10}$$

$$0 \leq L_{n,s,y} \leq D_n, \forall n \in N, s \in S, y \in Y\backslash\{2\}, (s,y) \in \mathbb{A}, \tag{C.11}$$

$$0 \leq L_{n,s,y} \leq L_{n,s,1}, \forall n \in N, s \in S\backslash\{0\}, y \in Y\backslash\{1\}, (s,y) \in \mathbb{A}, \tag{C.12}$$

$$L_{n,0,0} = 0, \forall n \in N, \tag{C.13}$$

$$P_g^{min} x_{g,s,y} \leq p_{g,s,y} \leq P_g^{max} x_{g,s,y} FC_g, \forall g \in G, s \in S \backslash \{0\}, y \in Y \backslash \{1\}, (s,y) \in \mathbb{A}, \quad \text{(C.14)}$$

$$p_{g,0,0} + r_{g,0,0}^{up} \leq P_g^{max} x_{g,0,0} FC_g, \forall g \in G, \quad \text{(C.15)}$$

$$p_{g,0,0} - r_{g,0,0}^{down} \geq P_g^{min} x_{g,0,0}, \forall g \in G, \quad \text{(C.16)}$$

$$0 \leq r_{g,0,0}^{up} \leq r_g^{up,max}, \forall g \in G, \quad \text{(C.17)}$$

$$0 \leq r_{g,0,0}^{down} \leq r_g^{down,max}, \forall g \in G, \quad \text{(C.18)}$$

$$r_{g,s,y}^{up} = 0, \forall g \in G, s \in S \backslash \{0\}, \in Y \backslash \{0\}, \quad \text{(C.19)}$$

$$r_{g,s,y}^{down} = 0, \forall g \in G, s \in S \backslash \{0\}, \in Y \backslash \{0\}, \quad \text{(C.20)}$$

$$\sum_{g \in z} r_{g,0,0}^{up} \geq R_z^{up}, \forall z \in Z, \quad \text{(C.21)}$$

$$\sum_{g \in z} r_{g,0,0}^{down} \geq R_z^{down}, \forall z \in Z, \quad \text{(C.22)}$$

$$v_i \in \{0,1\}, \forall i \in I; x_{g,s,y} \in \{0,1\}, \forall g \in G, s \in S, y \in Y \backslash \{1\}, (s,y) \in \mathbb{A}, \quad \text{(C.23)}$$

where (C.1) represents the objective function to minimize, which is similar to the model presented in Appendix B but adding the network infrastructure investment costs, (C.2) represents the nodal balance incorporating the flows through the new network infrastructure, and (C-7) - (C.9) represent the angular coupling, losses and thermal limits of this new infrastructure. All other constraints are the same as presented in Appendix B.

References

Alvarado, D., Moreira, A., Moreno, R., & Strbac, G. (2018). Transmission network investment with distributed energy resources and distributionally robust security. *IEEE Transactions on Power Systems, 34*(6), 5157-5168.

Alvarado, D., Moreno, R., Orchard, M., & Kirschen, D. (2022). Cost-benefit analysis of maintenance plans: Case study of the power system of a large industrial facility. *IEEE Transactions on Power Systems*, Early Access, 1-12.

Asamov, T., & Powell, W. (2018). Regularized decomposition of high-dimensional multistage stochastic programs with markov uncertainty. *SIAM Journal on Optimization, 28*(1), 575-595.

Billington, R., & Allan, R. (1984). *Reliability evaluation of power systems.* New York and London: Plenum Press.

Cain, M. B., O'Neill, R. P., & Castillo, A. (2012). *History of optimal power flow and formulations.* Retrieved from https://www.ferc.gov/sites/default/files/2020-05/acopf-1-history-formulation-testing.pdf

Capitanescu, F., Martinez-Ramos, J., Panciatici, P., Kirschen, D., Marano-Marcolini, A., Platbrood, L., & Wehenkel, L. (2011). State-of-the-art, challenges, and future trends in security constrained optimal power flow. *Electric Power Systems Research, 81*(8), 1731-1741.

Chen, Y., Moreno, R., Strbac, G., & Alvarado, D. (2018). Coordination strategies for securing AC/DC flexible transmission networks with renewables. *IEEE Transactions on Power Systems, 33*(6), 6309-6320.

Coordinador Electrico Nacional. (2018). *Estudio de restricciones en el sistema de transmision.* Retrieved from https://acortar.link/0Gvj38

Coordinador Electrico Nacional. (2018). *Informe definitivo estudio de continuidad de suministro.* Retrieved from https://acortar.link/0Gvj38

Coordinador Electrico Nacional. (2019). *Documentos de modelacion del SEN*. Retrieved from https://www.coordinador.cl.

Cordera, F., Moreno, R., & Ordóñez, F. (2023). Unit commitment problem with energy storage under correlated renewables uncertainty. *Operations Research, 71*(6), 1960-1977.

He, J., Cheng, L., Kirschen, D., & Sun, Y. (2011). Optimising the balance between security and economy on a probabilistic basis. *Generation, Transmission & Distribution, IET, 4*(12), 1275-1287.

Hedman, K., O'Neill, R., Fisher, E., & Oren, S. (2009). Optimal transmission switching with contingency analysis. *IEEE Transactions on Power Systems, 24*(3), 1577-1586.

Hu, B., Xie, K., & Tai, H.-M. (2018). Inverse problem of power system reliability evaluation: Analytical model and solution method. *IEEE Transactions on Power Systems, 33*(6), 6569-6578.

Joskow, P. (2006). Patterns of transmission investments. In P. Joskow, *Competitive Electricity Markets and Sustainability.* François Lévêque.

Krishnan, V., Ho, J., Hobbs, B., Liu, A., McCalley, J., Shahidehpour, M., & Zheng, Q. (2016). Co-optimization of electricity transmission and generation resources for planning and policy analysis: Review of concepts and modeling approaches. *Energy Systems, 7*(2), 297-332.

Ministerio de Energia Chile. (2015). *Energia 2050 politica energetica de chile.* Retrieved from https://www.energia.gob.cl/sites/default/files/energia_2050_-_politica_energetica_de_chile.pdf

Ministerio de Energia Chile. (2017). *Decreto 6 T.* Retrieved from https://www.bcn.cl/leychile/navegar?idNorma=1123617&idParte=

Ministerio de Energia Chile. (2018). *Resolucion exenta 227.* Retrieved from https://acortar.link/0Gvj38

Monticelli, A., Pereira, M., & Granville, S. (1987). Security-constrained optimal power flow with post-contingency corrective rescheduling. *IEEE Transactions on Power Systems, 2*(1), 175-180.

Moreno, R., Pudjianto, D., & Strbac, G. (2013). Transmission network investment with probabilistic security and corrective control. *IEEE Transactions on Power Systems, 28*(4), 3935-3944.

Niu, T., Li, F., Hu, B., Lu, H., Peng, L., Xie, K., . . . Zhou, K. (2021). Research on the inverse problem of reliability evaluation–model and algorithm. *IEEE Access, 9*, 12648-12656.

Panteli, M., & Mancarella, P. (2015). Influence of extreme weather and climate change on the resilience of power systems: Impacts and possible mitigation strategies. *Electric Power Systems Research,*

127, 259-270. Retrieved from https://www.sciencedirect.com/science/article/pii/S037877961500187X

Rodrigues, A., & Silva, M. (2013). Confidence intervals estimation for reliability data of power distribution equipments using bootstrap. *IEEE Transactions on Power Systems, 28*(3), 3283-3291.

Stott, B., & Alsac, O. (2012). Optimal power flow - Basic requirements for real-life problems and their solutions. *In SEPOPE XII Symposium, Rio de Janeiro, Brazil*.

Strbac, G., Kirschen, D., & Moreno, R. (2016). Reliability standards for the operation and planning of future electricity networks. *Foundations and Trends® in Electric Energy Systems, 1*(3), 143-219.

Zhang, H., Vittal, V., Heydt, G., & Quintero, J. (2012). A mixed-integer linear programming approach for multi-stage security-constrained transmission expansion planning. *IEEE Transactions on Power Systems, 27*(2), 1125-1133.

Zhang, J., & Sanderson, A. (2009). *Adaptive differential evolution: A robust approach to multimodal problem optimization.* Springer Science & Business Media.